Journal of Operation and Automation in Power Engineering

Vol. 7, No. 2, Oct. 2019, Pages: 196-205

http://joape.uma.ac.ir

The Effect of High Penetration Level of Distributed Generation Sources on Voltage Stability Analysis in Unbalanced Distribution Systems Considering Load Model

M. Kazeminejad[1], M. Banejad[1,], U. D. Annakkage[2], N. Hosseinzadeh[3]*

[1]*Department of Electrical and robotic Engineering, Shahrood University of Technology, Shahrood, Iran.*

[2]*Department of Electrical and Computer Engineering, University of Manitoba, Winnipeg, MB, Canada.*

[3]*Department of Electrical and Computer Engineering, Sultan Qaboos University, Muscat 123, Sultanate of Oman.*

Abstract- *Static voltage stability is considered as one of the main issues for primary identification before voltage collapsing in distribution systems. Although, the optimum siting of distributed generation resources in distribution electricity network can play a significant role in voltage stability improving and losses reduction, the high penetration level of them can lead to reduction in the improvement of load-ability. Moreover, the rapid variation and types of loads in distribution networks will have a significant impact on the maximum load-ability across the whole system. In this paper, a modified voltage stability index is presented with regard to distributed generation units (DG) along with two-tier load model. By applying the Imperialist Competition Algorithm (ICA), the best size of DG with corresponding of DG placement is used to improve the voltage stability and reducing the losses. It is shown in the paper that the DG penetration level can have influence on load-ability of the system and also the voltage regulators performance. The simulation results on the standard IEEE-13 Bus test feeder illustrate the precision of studies method and the load-ability limits in the system, taking into account the high penetration level of distributed generation units.*

Keyword: Modified voltage stability index, Maximum load-ability, Distributed generation penetration level, Load modelling.

1. INTRODUCTION

Today, distribution systems have faced the high penetration level of the distributed generations (DGs) due to increasing of load demand, solving the environmental problems and development of current DG structures. The reduction of losses, voltage stability improvement, power quality and network security enhancements are among the other benefits of DG units. To achieve these benefits, the siting and sizing of the distributed generation sources have been considered by many researchers [1-2]. Also, some researchers showed that the presence of DGs can reduce the consumer's payments, therefore from a financial point of view, the penetration of DG is advisable [3]. In spite of the above advantages, increasing the penetration of DG units itself results in negative effects on distribution systems such as over voltages [4-5] and interference with voltage regulation [6] and may even reduce the voltage stability depending on the of DG operating performance (with unity, lagging or leading power factors) [7]. Another investigation is studied in Ref. [8[which discusses about high penetration of DG in complement to load tap changers (LTC) in order to keep distribution electricity networks (DEN) voltages within desired limits. It is observed that increasing the reactive powers of DG in order to support DEN voltages decrease the number of LTC steps and consequently, the power factor at transmission/distribution connection point will improve. The impact of reverse power flow due to DG penetration level is investigated in Ref. [9]. They revealed that the step-type voltage regulator (SVR) will reduce the tap to lower the voltage, if the source side voltage is greater than the SVR set-point voltage. Also, this sequence may continue until unacceptable operation with DG, where the regulator taps reach to minimum tap.

The importance of voltage stability studies in DEN is becoming more important due to the rapid growth of the use of distributed generators, as well as high R to X ratio characteristic of the distribution feeders, which can lead to voltage collapse phenomenon before reaching to the maximum load-ability. It means that if the distribution system is not considered in the voltage stability studies,

Received: 14 Jan. 2019
Revised: 09 Feb. and 04 Apr. 2019
Accepted: 11 May 2019
*Corresponding author:
E-mail: m.banejad@gmail.com (M. Banejad)
Digital object identifier: 10.22098/joape.2019.5726.1427
Research Paper

this will result in errors in determination of the maximum load-ability of the system [10]. Since most power systems are very close to their critical operating limit to provide the required network power, the maintaining of the network at high levels of security is important [11]. Therefore, the correct knowledge of the current system's performance is necessary to assess the voltage stability.

Many analytical methods have been studied for the evaluation of voltage instability and the prediction of voltage collapse. In Ref. [12], a static voltage stability evaluation is investigated which used two-point estimation method and continuation power flow in DEN considering the stochastic DG units. A non-linear three-phase maximum load-ability model with wind power generation and load forecasting deviation is presented in Ref. [13] in order to evaluate probabilistic static voltage stability. They showed that the proposed method has ability to assess system reliability - compared with deterministic power flow methods. The author presented the voltage stability enhancement and power loss reduction in power system by optimizing the size and location of static VAR compensator devices, using fuzzy weighted seeker optimization algorithm [14]. In Ref. [15], two voltage stability indicators based on Chakrovorty index [16] and smart grid infrastructures are described in radial networks. However, these indicators depend only on the bus voltages. Voltage stability assessment has been mainly classified into three categories [17-18]: A)Voltage stability analysis and prediction of voltage collapse based on P-V and P-Q curves, eigenvalues analysis, modal analysis and energy function; B) Voltage stability analysis to determine the weak buses including voltage stability indexes defined by L index and voltage stability index (VSI); C) Voltage stability analysis to identify the weak branches including fast voltage stability index (FVSI), linear voltage stability index (L_{mn}), voltage collapse prediction index (VCPI) and line quality proximity (LQP). Among all the mentioned categories, two cases B and C are used more in the analysis of the voltage stability of distribution systems and in determining the system load-ability due to their simplicity in expressing relationships quantitatively.

In order to analyze the voltage stability in unbalanced distribution systems using the above-described indices, different generalized load flow techniques such as Newton-Raphson [19], a fast decoupled method [20] and the backward/forward sweep method [11] have been carried out in the three-phase networks. Among them all, the backward/forward sweep method has been of interest for many researchers due to the high convergence rate and the radial nature of the conventional DEN. However, in most of these studies, the load model is generally used as a constant power, while it has been shown that load models can significantly affect the location and size of the DG sources as well as voltage stability in distribution systems [18, 21].

The main contributions of this paper are as follows:

- The definition of a modified voltage stability index is developed to identify the weak buses in a three-phase distribution system and eventually of the load-ability of unbalanced DEN are obtained. For this purpose, a two-bus equivalent system is used to analyze the proposed index in order to compare with other indicators.
- The evaluation of voltage stability on the IEEE 13-bus standard DEN performed with consideration of DG units. In order to examine the DG effect, the optimum siting and sizing of DG are considered with the Imperialist Competition Algorithm (ICA). Hence, the effects of the DG operating with the load model are studied in the voltage stability analysis of the distribution systems in terms of three different DG performance conditions (unity power factor, lagging and leading power factors).
- The two-tier load model is used to evaluate the load model in voltage stability analysis where the buses voltage magnitude is affected by active and reactive power loads.
- Similarly, the effect of penetration level on the voltage stability and maximum load-ability as well as it's interference with voltage regulators are studied in this paper.

This paper is organized as follows: The mathematical model of voltage stability index considering load model and DG units is reviewed in Section 2. The optimization method for siting and sizing of DG is presented in Section 3. Simulation results and the impact of high penetration level of DGs are illustrated in Section 4. Finally, Section 5 concludes the paper.

2. MODIFIED VOLTAGE STABILITY INDEX CONSIDERING DG AND LOAD MODEL

Some critical issues of a distribution system, such as a load model and effect of on-load tap changer transformer (OLTC) are important in analyzing the voltage stability. Since the static load model is effective and sufficient in studying the static voltage stability, in this paper the static load model of ZIP and two-tier load model have been used.

2.1. Load Model

DEN load modeling is typically a complex task that requires detailed model, behavior, types and power consumption rates of the loads. Most of the research undertaken in the optimal location plans and optimal size of DGs usually use load flow programs that typically utilize positive sequence models [5, 7]. Therefore, lack of using a comprehensive study may lead to inconsistent and inaccurate results in siting and sizing of the renewable resources in the distribution systems.

Nowadays, researchers in the voltage stability areas try to use typical load models [18, 21, 22]. These studies typically define the active and reactive power at any instant of time as a function of bus voltage magnitudes and frequency load models in the static voltage stability studies such as polynomial and exponential load models. As the polynomial load models (ZIP) cannot perfectly model the fast losing of load when bus voltage decreases bellow 0.7 p.u., the two-tier load model is performed to solve this problem which considers the load model as clearly described in [23]. In this case, each load is modeled as a ZIP model when the voltage is near the rated voltage, and when voltage magnitude lies in the range of 0.3 p.u. to 0.7 p.u, the load is modelled as a constant impedance model.

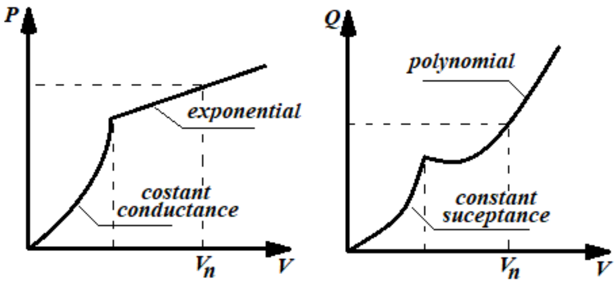

Fig. 1. Two-tier load model [23].

The ZIP load model can be expressed by constant impedance, constant current and constant power loads as below [24].

$$P = P_{0_i}[\alpha_1|\overline{V_i}|^2 + \alpha_2|\overline{V_i}| + \alpha_3] * \lambda \tag{1}$$

$$Q = Q_{0_i}[\beta_1|\overline{V_i}|^2 + \beta_2|\overline{V_i}| + \beta_3] * \lambda \tag{2}$$

where α_j (j = 1, 2, 3) is considered as the portions of constant impedance, constant current and constant power loads, respectively and β_j is considered as the coefficients of reactive power load proportions. $\overline{V_i}$ is the voltage amplitude of bus i, and P_0 and Q_0 are the value of nominal active power and reactive power, respectively. The coefficient λ is considered as the load-ability which is defined from the value of zero to the maximum loading value (λ_{max}).

2.2. Modeling of the distributed generation unit

Principally, the distributed generation units include three types of control structures in forms of PV bus control mode, current mode and load bus (or so-called PQ) mode. The bus connected to the DG with PV control mode can be modeled as PV bus. However, for a connected DG operating in current control mode and PQ mode, this bus is typically modeled as PQ bus. It has been shown that the use of DG to regulate the voltage level in the distribution system can conflict with other devices like voltage regulators in the grid [25]. It should be noted that DG modeling with PQ control mode and controlled reactive power injections are valid because a DG (such as wind turbines and photovoltaic units) is connected to the network through electronic interfaces [7]. In this research, the dispersed generation unit is assumed to operate in the PQ control mode which is based on the electronic interface of the inverter.

Also, the selection of DG unit in the DEN is often based on constant power factor to minimize interference with the voltage regulators in the system [26]. In this study, the DG is assumed to be in three forms of active power injection, active and reactive power injections and active power injected with reactive power absorption. Since the DG placement and sizing are effective in solving the voltage stability problem, a new method is proposed in the following section to optimize the size and location of DG in order to improve the voltage stability index.

2.3. Modified voltage stability index (MVSI)

First, it is considered that the equivalent circuit seen from each bus of distribution system is shown in Fig. 2. The DG is assumed to be located in receiving bus operating at unity power factor. The principal voltage equation for phase *i* can be written as below

$$\vec{V}_{R,i} = \vec{V}_{S,i} - \vec{Z}_{eq}.\vec{I}_{R,i} \tag{3}$$

where *i* refers to the phase type and can be a, b or c. It should be noted that as an unbalanced condition is studied in this paper, the subscript *i* is inserted in Eq. (3). In this regard, the expanded form of Eq. (3) can be written as follow

$$\begin{bmatrix}\vec{V}_{R,a}\\ \vec{V}_{R,b}\\ \vec{V}_{R,c}\end{bmatrix} = \begin{bmatrix}\vec{V}_{S,a}\\ \vec{V}_{S,b}\\ \vec{V}_{S,c}\end{bmatrix} - \begin{bmatrix}Z_{aa} & Z_{ab} & Z_{ac}\\ Z_{ba} & Z_{bb} & Z_{bc}\\ Z_{ca} & Z_{cb} & Z_{cc}\end{bmatrix}.\begin{bmatrix}\vec{I}_{R,a}\\ \vec{I}_{R,b}\\ \vec{I}_{R,c}\end{bmatrix} \tag{4}$$

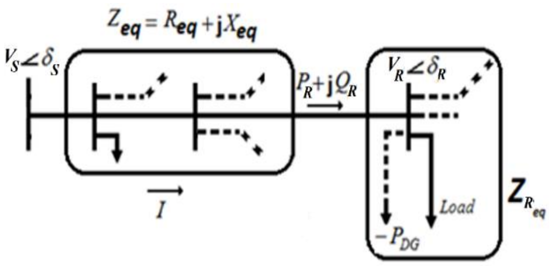

Fig. 2. Equivalent circuit seen from each bus of the DEN

Substituting $\vec{I}_{R,i} = \left(\frac{P_{R,i}+jQ_{R,i}}{\vec{V}_{R,i}}\right)^*$ in the principal voltage equation and separating the real and imaginary parts, result:

$$V_{S,i}V_{R,i}Cos(\delta_i) = |V_{R,i}|^2 + \left[R_{eq,i}\left(P_{R,i} - P_{DG,i}\right) + X_{eq,i}Q_{R,i}\right] \tag{5.a}$$

$$V_{S,i}V_{R,i}Sin(\delta_i) = \left[X_{eq,i}\left(P_{R,i} - P_{DG,i}\right) - R_{eq,i}Q_{R,i}\right] \tag{5.b}$$

where δ_i is the difference between the angles of the sending bus voltage (V_S) and the receiving bus voltage (V_R) for phase i ($\delta_i = \delta_{s,i} - \delta_{R,i}$) . Also, in this analysis, the first bus is considered as the reference bus with fixed magnitude voltage. P_R and Q_R are the total active and reactive power received by the receiving bus in the distribution system, respectively. R_{eq} and X_{eq} are also the resistance and reactance equivalent to the radial distribution line from the beginning of the feeder to the power receiving bus, respectively calculated as follows:

$$\left(P_{s,i} + jQ_{s,i}\right) - \left(P_{R,i} + jQ_{R,i}\right) = \left(R_{eq,i} + jX_{eq,i}\right) * \left|\vec{I_i}\right|^2 \tag{6}$$

By calculating $\overline{I_i} = \left(\frac{\vec{V}_{S,i}-\vec{V}_{R,i}}{R_{eq,i}+jX_{eq,i}}\right)$ and solving of above equations, gives:

$$R_{eq,i} + jX_{eq,i} = \frac{\left[\left(P_{s,i} - P_{R,i}\right) + j\left(Q_{S,i} - Q_{R,i}\right)\right] * \left|\vec{V}_{S,i} - \vec{V}_{R,i}\right|^2}{\left[\left(P_{s,i} - P_{R,i}\right)^2 + \left(Q_{S,i} - Q_{R,i}\right)^2\right]} \tag{7}$$

Eliminating the angle δ_i from Eq. (5.a) and Eq. (5.b),

$$|V_{R,i}|^4 + \left\{2\left[R_{eq,i}\left(P_{R,i} - P_{DG,i}\right) + X_{eq,i}Q_{R,i}\right] - |V_{s,i}|^2 + \left\{\left(R_{eq,i}^2 + X_{eq,i}^2\right)\left[\left(P_{R,i} - P_{DG,i}\right)^2 + {Q_{R,i}}^2\right]\right\} = 0 \tag{8}$$

More simplifications results:

$$|V_{R,i}|^2 = \frac{\left\{|V_{s,i}|^2 - 2\left[R_{eq,i}\left(P_{R,i} - P_{DG,i}\right) + X_{eq,i}Q_{R,i}\right]\right\} \pm \sqrt{\Delta}}{2} \tag{9.a}$$

$$\Delta = \left\{2\left[R_{eq,i}\left(P_{R,i} - P_{DG,i}\right) + X_{eq,i}Q_{R,i}\right] - |V_{s,i}|^2\right\}^2 - 4\left\{\left(R_{eq,i}^2 + X_{eq,i}^2\right)\left[\left(P_{R,i} - P_{DG,i}\right)^2 + {Q_{R,i}}^2\right]\right\} \tag{9.b}$$

Regarding the issue that $|V_{R,i}|^2 \geq 0$,

$$\left\{|V_{s,i}|^2 - 2\left[R_{eq,i}\left(P_{R,i} - P_{DG,i}\right) + X_{eq,i}Q_{R,i}\right]\right\} \pm \sqrt{\begin{array}{l}\left\{2\left[R_{eq,i}\left(P_{R,i} - P_{DG,i}\right) + X_{eq,i}Q_{R,i}\right] - |V_{s,i}|^2\right\}^2 \\ -4\left\{\left(R_{eq,i}^2 + X_{eq,i}^2\right)\left[\left(P_{R,i} - P_{DG,i}\right)^2 + {Q_{R,i}}^2\right]\right\}\end{array}} > 0 \tag{10}$$

It can be understood that the first term of the left hand side of (10) should be greater than zero,

$$\left\{|V_{s,i}|^2 - 2\left[R_{eq,i}\left(P_{R,i} - P_{DG,i}\right) + X_{eq,i}Q_{R,i}\right]\right\} > 0$$
$$\text{or, } 2\left[R_{eq,i}\left(P_{R,i} - P_{DG,i}\right) + X_{eq,i}Q_{R,i}\right] - |V_{s,i}|^2 < 0 \tag{11}$$

Also, to obtain the practical result, Δ must be greater or equal than zero ($\Delta \geq 0$). According to Eq. (9.a) and Eq. (11), two acceptable voltages can be obtained for V_R. Fig. 3. Shows the concept of two voltages solution on the PV curve.

$$\left\{2\left[R_{eq,i}\left(P_{R,i} - P_{DG,i}\right) + X_{eq,i}Q_{R,i}\right] - |V_{s,i}|^2\right\}^2 \geq 4\left\{\left(R_{eq,i}^2 + X_{eq,i}^2\right)\left[\left(P_{R,i} - P_{DG,i}\right)^2 + {Q_{R,i}}^2\right]\right\} \tag{12}$$

Hence,

$$\left\{2\left[R_{eq,i}\left(P_{R,i} - P_{DG,i}\right) + X_{eq,i}Q_{R,i}\right] - |V_{s,i}|^2\right\} \geq 2\sqrt{\left(R_{eq,i}^2 + X_{eq,i}^2\right)\left[\left(P_{R,i} - P_{DG,i}\right)^2 + {Q_{R,i}}^2\right]} \tag{13.a}$$

$$\left\{2\left[R_{eq,i}\left(P_{R,i} - P_{DG,i}\right) + X_{eq,i}Q_{R,i}\right] - |V_{s,i}|^2\right\} \leq -2\sqrt{\left(R_{eq,i}^2 + X_{eq,i}^2\right)\left[\left(P_{R,i} - P_{DG,i}\right)^2 + {Q_{R,i}}^2\right]} \tag{13.b}$$

From Eq. (11) and Eq. (13), it can approve that Eq. (13.b) is the only acceptable answer. Therefore, by displacing the inequality of (13.b), we can obtain a modified voltage stability index with the presence of DG as follows, (9.a)

$$MVSI_i = \frac{2\left[R_{eq,i}\left(P_{R,i} - P_{DG,i}\right) + X_{eq,i}Q_{R,i}\right] + 2\sqrt{\left(R_{eq,i}^2 + X_{eq,i}^2\right)\left[\left(P_{R,i} - P_{DG,i}\right)^2 + {Q_{R,i}}^2\right]}}{|V_{s,i}|^2} \leq 1 \tag{14}$$

The distribution system studied will be stable when the value of defined index for each bus in all phases is less than one ($0 \leq MVSI_i < 1$). This voltage stability indicator is dimensionless and as a result, both actual and per-unit values can be used.

3. OPTIMIZATION TECHNIQUE

To maximize the benefits of using dispersed generation units in the distribution system, proper size and optimal DG placement are needed. Due to outstanding aspects of ICA such as high speed convergence, this optimization method is used along with the backward/forward sweep load flow in unbalanced radial distribution electricity network [27-28].

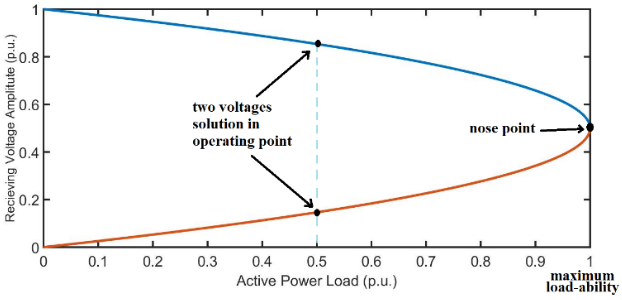

Fig. 3. Two voltage solutions and PV curve.

3.1. Problem formulation for siting and sizing of DG

In this section, the problem of finding the optimal size and proper location for DG installation is addressed by improving the voltage stability indicator presented in the previous section regarding the reduction of power losses in the distribution system. For this purpose, the DG is assigned to the buses which have the highest values of the voltage stability index. In the algorithm illustrated in flowchart of Fig.4, the size of DG is increased incrementally to achieve the lowest value of the objective function.

3.2. The proposed objective function

In this study, the proposed objective function is to optimize the DG capacity by minimizing the total power loss of power lines and improving the voltage stability index simultaneously, as follows:

$$f = min\left\{\left(\sum_{k=1}^{nb}\left(R_{k,a}\left|\bar{I}_{k,a}\right|^2 + R_{k,b}\left|\bar{I}_{k,b}\right|^2 + R_{k,c}\left|\bar{I}_{k,c}\right|^2\right)\right) + MVSI_i\right\} \tag{15}$$

Subject to

$$0 \le P_{DG} \le \frac{25}{100}\sum_{j=1}^{n} P_{Load,j} \tag{16}$$

where nb is the number of the distribution system branches, n is the number of buses, P_{DG} is the active power injected by the distributed generation unit and P_{Load} is the active power loads connected to each bus. The voltage magnitude in the beginning of the feeder (considered as an infinite bus) is set to 1.00(p.u.) with an angle of 0 degree. The voltage range for other buses are considered as

$$V_{j,min} \le V_j \le V_{j,max} \qquad ,j = 2,\dots n \tag{17}$$

The voltage constraints for $V_{j,max}$ and $V_{j,min}$ are 1.05 (p.u.) and 0.9(p.u.), respectively.

3.3. The procedure for siting and sizing of DG

After applying the backward/forward sweep load flow method and determining the critical buses near to the voltage instability, incremental step size of DG for critical buses are implemented separately. After completing the steps for all buses that are prone to DG installation, the selected bus with the optimum size of DG will be chosen under the lowest value of the proposed objective function from the database. At this stage, it is assumed that DG unit has a unit power factor.

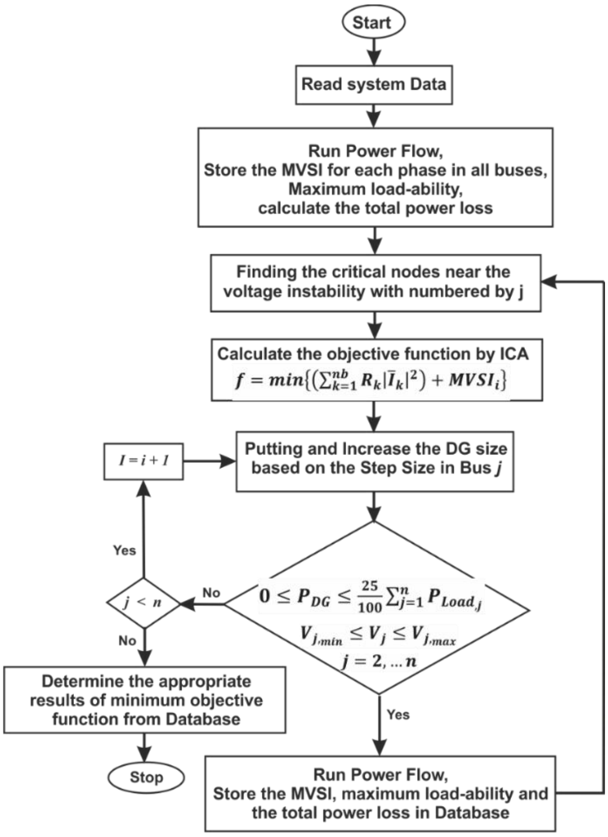

Fig. 4. Optimization schedule flowchart for allocation and size of DG

4. SIMULATION AND RESULT

In order to verify the correctivenes of the proposed index in voltage stability assessment in comparison to couple of different indicators, a simulation has been performed on the two bus equivalent system shown in Fig. 2.

The fast voltage stability index (FVSI) given in Ref. [29] is presented as (18), which depends only to reactive power load.

$$FVSI = \frac{4\left|Z_{eq,i}\right|^2 Q_{R,i}}{X_{eq,i}\left|V_{S,i}\right|^2} \tag{18}$$

Therefore, with variation of the active power load in receiving buses (especially in DGs having unit power factor), this method cannot be used. Hence, FVSI will not be applicable to be used in voltage analysis in DNO. Also, the power stability index (PSI) which was defined by Amman [30] has some inaccuracies.

$$PSI = \frac{4R_{eq,i}\left(P_{R,i} - P_{DG,i}\right)}{\left|V_{S,i}\right|^{2} cos^{2}(\theta_i - \delta_i)} \quad (19)$$

where $\delta_i = \delta_{S,i} - \delta_{R,i}$ and $\theta_i = \arctan(\frac{X_{eq,i}}{R_{eq,i}})$.

PSI varies from 0 (no loading) to 1 (collapse point) when $\left(P_{R,i} - P_{DG,i}\right) > 0$. If $\left(P_{R,i} - P_{DG,i}\right) \leq 0$, PSI becomes negative or zero, which shows the system always has a stable voltage. The comparison between these indicators and proposed MVSI is given as follow.

In Fig. 2, it is assumed that $V_S\measuredangle\delta_S = 1.00\measuredangle 0.0\ (p.u.)$, and as an example, impedance assumed as $R_{eq} + jX_{eq} = 0.05 + j0.1\ (p.u.)$. The values of load demand at load initial condition are assumed as $P_R + jQ_R = 0.5 + j1.0\ (p.u.)$. Tables 1, 2 and 3 present two voltage solutions at the receiving bus for each iteration, which express the PV curve. The three voltage indicators MVSI, FVSI and PSI are calculated when the load is gradually increased. λ represents as load-ability factor with regard to its initial value of load. Table 1 shows the results when both active and reactive power loads are increased with a constant power factor. It can be seen that at $\lambda = 2.00$, all indicators work properly. Table 2 shows the result when only the active power loads are increased. It can be understood that the FVSI is constant for all load-ability factors and it is not proper to use it for voltage stability. Also, the PSI reaches to its maximum value (voltage collapse point, PSI=1.00) at $\lambda = 3.845$; whereas the magnitude of two voltages solution at the receiving bus on PV curve still not reached to nose point. Table 3 shows the result when only the reactive power loads are increased. It is described that FVSI reaches to its maximum value with $\lambda = 2.00$; in while nose point doesn't happen. Also, the PSI doesn't work correctly and has an essential flaw; where the two voltage solutions reach together as a nose point of PV curve, but the value of PSI is 0.8834.

Table 1. DNS load-ability when both active and reactive power loads are increased with constant power factor

λ	PV Curve		MVSI	PSI [30]	FVSI [29]
	V_{High}(p.u.)	V_{Low}(p.u.)			
1.0000	0.8535	0.1464	0.5000	0.5000	0.5000
1.4776	0.7555	0.2444	0.7388	0.7388	0.7388
1.8927	0.6158	0.3842	0.9463	0.9463	0.9463
2.0000	0.5000	0.5000	1.0000	1.0000	1.0000

Table 2. DNS load-ability only by increasing of active power load

λ	PV Curve		MVSI	PSI [30]	FVSI [29]
	V_{High}(p.u.)	V_{Low}(p.u.)			
1.0000	0.8535	0.1464	0.5000	0.5000	0.5000
1.8927	0.8185	0.1880	0.6025	0.7714	0.5000
2.6521	0.7816	0.2376	0.7040	0.9121	0.5000
3.8443	0.6981	0.3470	0.8767	1.0000	0.5000
4.6602	0.5324	0.5324	1.0000	---	0.5000

Table 3. DNS load-ability only by increasing of reactive power load

λ	PV Curve		MVSI	PSI [30]	FVSI [29]
	V_{High}(p.u.)	V_{Low}(p.u.)			
1.0000	0.8535	0.1464	0.5000	0.5000	0.5000
1.3125	0.8059	0.1948	0.6266	0.5414	0.6562
1.7011	0.7325	0.2706	0.7867	0.6130	0.8505
2.0000	0.6519	0.3535	0.9110	0.7025	1.0000
2.2132	0.5037	0.5037	1.0000	0.8834	---

4.1. The Case study

The studied system is an unbalanced IEEE 13 Bus Test Feeder with 4.16 kV and a total Spot Load of 3266 kW, 1986 kVAr and distributed load of 200 kW, 116 kVAr, one tap changer transformer and one transformer 4.16 kV/0.48 kV and also, 2 capacitive banks in buses 13 and 10 according to fig.5. The details of power lines and loads data are presented in Ref. [31].

In this study, some assumptions have been made for simulations. Take, for example, ignoring limited thermal capacity and the susceptance of lines. In addition, it is assumed that the magnitude voltage of the first bus is 1.00 p.u. Also, the position of transformer taps are included for each phase individually regarding that taps range will be 10 steps.

4.2. The effect of transformer taps on voltage stability

Figure 6 shows the voltage profile of phases A to C for three cases; normal load, increasing the load-ability by fixing the transformer taps obtained from the previous state (the values of 6, 5 and 6 for phases A, B and C, respectively), and increasing the load-ability in condition of changing the transformer taps. The results describe the voltage instability condition due to an increase in load-ability to ($\lambda_{max} = 1.3$), while the taps position of transformer are fixed to 6, 5, 6 for three phases. Also, considering the flexibility of the transformer tap changer in the specified range, it can be seen that the voltage profile and therefore the voltage stability margin are significantly improved.

Figure 7 shows the status of the modified voltage stability index for all three proposed cases. It is shown that when the maximum load-ability condition occurs, the index amount reaches its critical value, i.e., the value one in the critical bus 7, which means that the voltage collapse occurred.

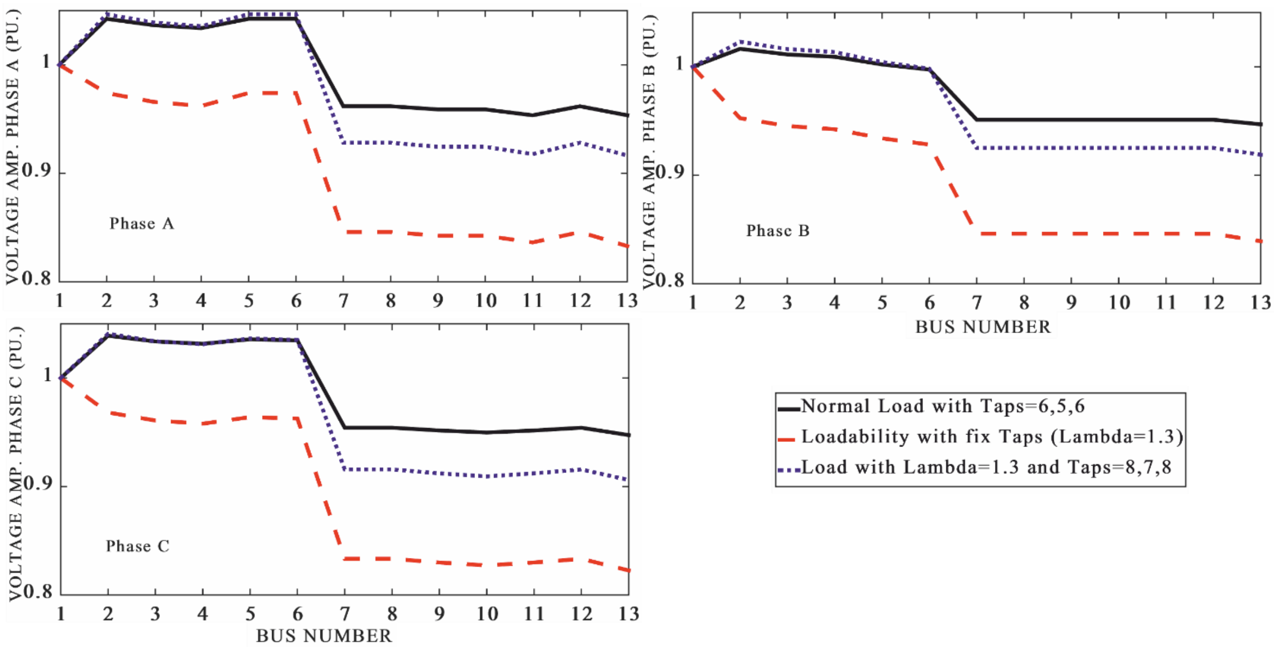

Fig. 6. voltage profiles of three phase for maximum load-ability; i) Phase A , ii) Phase B , iii) Phase C

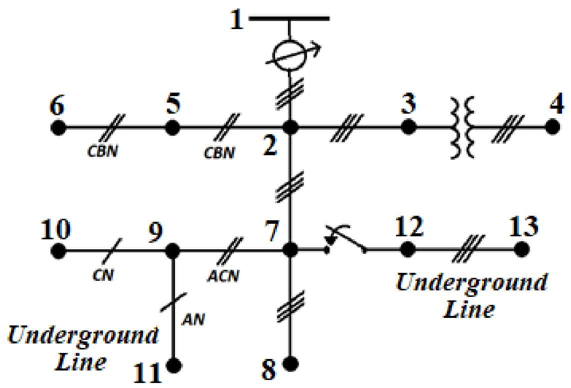

Fig. 5. IEEE13bus distribution test system

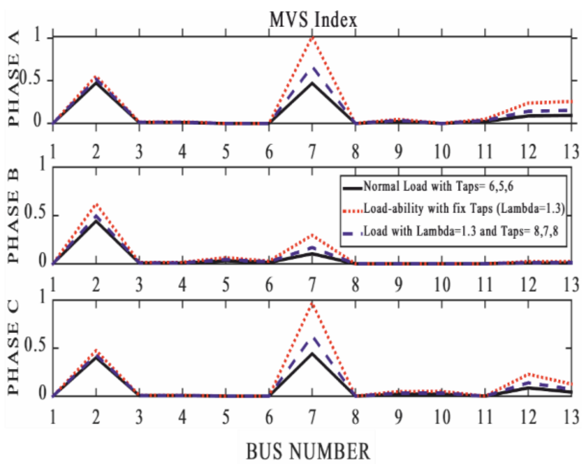

Fig. 7. Three-phase voltage stability index for maximum load-ability

4.3. The effect of optimized DG siting on the voltage stability

Based on the optimization algorithm defined in the section three, the bus number 13 is identified as the best location for DG installation. Figure 8 shows the power loss reduction due to optimal DG siting in bus 13 in which the total active power loss is decreased approximately 40%. Table 4 shows the optimal DG size and total losses of the whole system containing the transformer taps in each phase. It can be observed that the total amount of active power loss decreases from 213.42MW to 127.46MW as transformer tap is set to 5 for all phases. Also, the voltage profile for the phase B is shown in Fig. 9 excluding the DG and with optimum size of DG in normal load case that is observed with considering the optimal DG, the voltage profile is significantly improved.

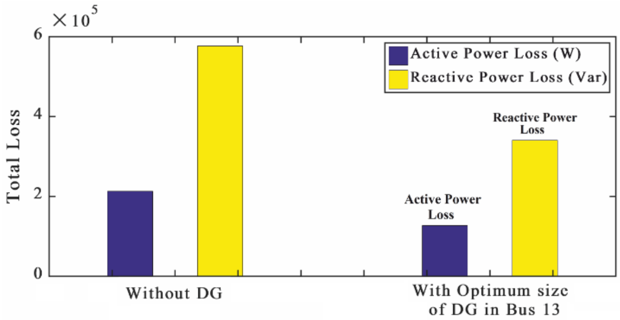

Fig. 8. System power losses with / without optimal DG

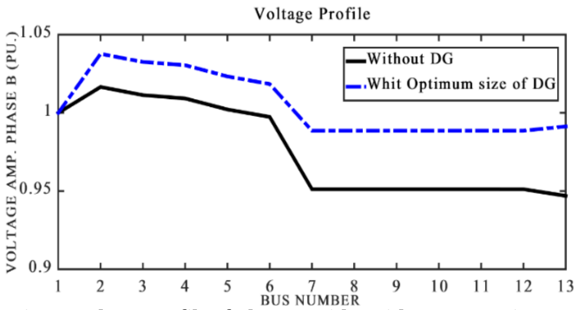

Fig. 9. Voltage profile of phase B with / without DG optimum size

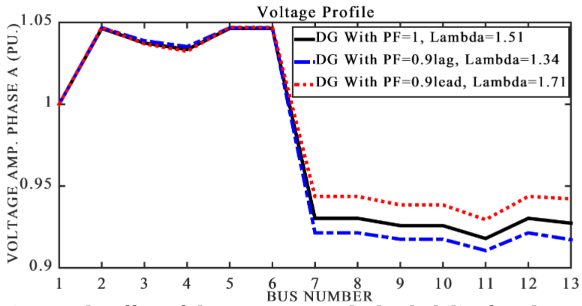

Fig. 11. The effect of the DG types on the load-ability for Phase A

Table 4. System power losses with / without DG and transformer taps status

	Bus Number	Size (kW)	Active power loss (kW)	Reactive power loss (kVar)	Transformer taps status		
					Phase a	Phase b	Phase c
Without DG	---		213.42	576.61	6	5	6
With optimal DG	13	288.83	127.46	340.11	5	5	5

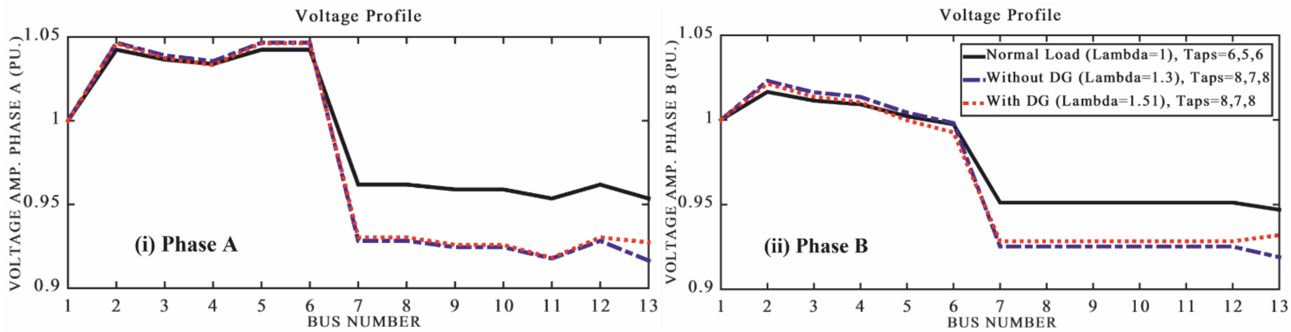

Fig. 10. The load-ability effect on the voltage profile (i) phase A, and (ii) phase B; with / without DG

The voltage profiles in Fig. 10 illustrate a comparison of the impact of the load-ability for three cases; normal load conditions with and without the DG installation for the two phases A and B. Without DG, the maximum load-ability reaches to $\lambda_{max} = 1.3$ with a change in the tap position of the transformers to 8, 7 and 8 for A, B and C phases, respectively. It is also shown that with the optimized DG siting in Bus 13, the system load-ability increases to $\lambda_{max} = 1.51$.

The influence of the DG types on load-ability of phase A is depicted in Fig. 11 for three different modes of DG performance, active power injection with unit power factor (PF = 1), active and reactive power injections with 0.9 lagging PF and active power injected with reactive power absorption with 0.9 leading PF. The results demonstrate that if the DG is capable of injecting both active and reactive power simultaneously, the load-ability increases significantly to $\lambda_{max} = 1.71$. Also, if the DG operates in a lag power factor mode, a considerable reduction in the system load-ability occur ($\lambda_{max} = 1.34$).

4.4. The effect of DG high penetration level on voltage stability

In order to study the penetration level of distributed generations on the voltage stability in DEN, two critical buses 7 and 13 are separately selected for DG installation. In this case, the DG size is increased up to 80% of the total demanded load by step size of 5%. Then, for each step, the maximum load-ability and the sensitivity of load-ability to penetration level are presented. In order to analyze the sensitivity of load-ability to penetration level, the maximum load-ability difference for the two closest DG penetration levels per the maximum load-ability without DG installation is calculated. The tap positions of transformer is fixed to 6, 5, 6 for each step.

$$\Delta\lambda = \frac{\lambda_{max}(i) - \lambda_{max}(i-1)}{\lambda_{max}(Without\_DG)} \tag{20}$$

λ_{max} is the maximum load-ability and *i* refers to the step increment of DG penetration level in each step.

According to Table 5, the maximum load-ability (λ_{max}) rises by increasing the DG penetration level in distribution system. It can also be seen that for increasing the penetration level above 55%, the sensitivity of load-ability tends to decrease significantly in comparison with the lower DG penetration levels.

It means that if the DG is installed in critical bus 13, with an increase in penetration level to 45% of the total demanded load, the load-ability sensitivity reaches the highest rate equal to 7.69% compared with 40% of penetration level. Also, for the penetration level higher than 60% of the total demanded power, the sensitivity load-ability decreases. It is obtained that the sensitivity load-ability for 60% of penetration level is equal 6.92%. These results describe that the slope of maximum load-ability decreases by growing up the DG penetration level and the use of DG in these circumstances may be not justified.

Table 5. System load-ability and the DG penetration level at bus 13

DG penetration level (%)	λ_{max}	$\Delta\lambda(\%)$	Active power loss (kW)
0	1.3	0	4.3239
5	1.36	4.62	4.3536
10	1.44	6.15	4.5393
15	1.51	5.38	4.5879
20	1.59	6.15	4.6923
25	1.68	6.92	4.8528
30	1.77	6.92	4.9856
35	1.86	6.92	5.1024
40	1.95	6.92	5.2189
45	2.05	**7.69**	5.4406
50	2.15	7.69	5.7077
55	2.25	7.69	6.0534
60	2.34	6.92	6.4203
65	2.42	6.15	6.8371
70	2.48	4.62	7.2160
75	2.54	4.62	7.7973
80	2.57	2.31	8.2188

Table 6. System load-ability and the DG penetration level at bus 7

DG penetration level (%)	λ_{max}	$\Delta\lambda(\%)$	Active power loss (kW)
0	1.3	0	4.3239
5	1.36	4.62	4.3988
10	1.43	5.38	4.5324
15	1.51	6.15	4.7220
20	1.59	6.15	4.8703
25	1.67	6.15	4.9778
30	1.76	6.92	5.1411
35	1.85	6.92	5.2695
40	1.95	**7.69**	5.4636
45	2.05	7.69	5.6412
50	2.15	7.69	5.8183
55	2.25	7.69	6.0171
60	2.35	7.69	6.2667
65	2.43	6.15	6.4006
70	2.51	6.15	6.6502
75	2.57	4.62	6.8404
80	2.62	3.85	7.0979

The results of the sensitivity load-ability analysis for increasing the DG penetration level installed in the critical bus 7 are tabulated in table 6. It can be seen that the maximum sensitivity load-ability reaches to 40 % of penetration level (7.69%). This rate has been reduced for penetration levels above 60%, and the amount of sensitivity load-ability has decreased to 6.15% in 65% of penetration level.

4.5. The interaction effect of the transmission system on the distribution system load-ability

The transmission and distribution systems are physically connected to each other, but they are typically studied separately in the analysis of voltage stability assessment. Table 7 shows the interactive effect of the transmission system on the distribution system load-ability. In this analysis, it is assumed that the initial voltage of the distribution feeder connected to the transmission network decreases to 0.95 p.u. due to some constraints of the transmission system.

The first row of table 7 describe that the system load-ability increases from 1.3 to 1.51 by considering the DG unit and with the change in transformer tap positions to 8, 7 and 8 for each phase, individually. It is also observed that the load-ability decreases due to a voltage drop from 1.3 to 1.19, when the DG is not considered (column one). In this case, the transformer taps significantly increase in order to maintain the distribution voltage profile in the desired range. Although, in the presence of DG the load-ability has not made any significant change (column two), the tap positions of transformer increased to 9, 9 and 10 for each phase in order to maintain normal condition of voltage stability in the system.

Table 7. The interaction effect of the transmission system on the distribution system load-ability

Muximum Load-ability (λ_{max})	*Without DG*			*With optimal DG (PF=1)*			*With optimal DG (PF=0.9 lag)*		
	Phase a	*Phase b*	*Phase c*	*Phase a*	*Phase b*	*Phase c*	*Phase a*	*Phase b*	*Phase c*
V=1 p.u.	**1.3**			**1.51**			**1.34**		
Transformer taps status	6	5	6	8	7	8	8	7	8
V=0.95 p.u.	**1.19**			**1.52**			**1.36**		
Transformer taps status	9	8	9	9	9	10	9	9	10

5. CONCLUSIONS

In this research, a modified voltage stability index (MVSI) presented in an unbalanced three-phase DENs in presence of distributed generation units. It has been shown that by considering load model and best size of DG, a significant effect on the voltage profile and voltage stability in DEN can be achieved. In order to improve the voltage stability index and reduce the effects of transformer taps in the distribution system, the ICA optimization technique has been used to determine the sizing and siting of DG with loss reduction. Furthermore, the influence of DG penetration level on the system load-ability margin is analyzed. It has been described that the load-ability margin can be improved by DG penetration level. However, the speed rate of load-ability was significantly reduced with respect to increase in high DG penetration levels. Moreover, since the effect of the transmission system constraints is typically ignored on the voltage stability studies in the distribution system, the impact of the distribution system load-ability on the transmission system has been investigated. It has been shown that the voltage reduction of the transmission system has a negative effect on both the load-ability and the transformer tap positions in distribution system.

REFERENCES

[1] Y. M. Atwa, E. F. El-Saadany, M. M. A. Salama, R. Seethapathy, “Optimal renewable resources mix for distribution system energy loss minimization,” *IEEE Trans. Power Syst.,* vol. 25, no. 1, pp. 360-370, 2010.

[2] M. Ettehadi, H. Ghasemi, S. Vaez-Zadeh, “Voltage Stability-Based DG Placement in Distribution electricity networks,” *IEEE Trans. Power Del.,* vol. 28, no. 1, 2013.

[3] S. Ghaemi, K. Zare, “A New Method of Distribution Marginal Price Calculation in Distribution Networks by Considering the Effect of Distributed Generations Location on Network Loss”, *J. Oper. Autom. Power Eng.,* vol. 5, No. 2, Dec. 2017, Pages: 171-180.

[4] R. walling, et. al., “summary of distributed resources impact on power delivery systems,” *IEEE Trans. Power Del., vol.* 23, 2008.

[5] M. Thomson, D. G. Infield, “Network power flow analysis for a high penetration of distributed generation,” *IEEE Trans. Power syst.,* vol. 22, pp. 1157-1162, 2007.

[6] P.P. Barker, R.W. de Mello, “Determining the impact of Distributed generation on power systems: Part 1 —radial distribution systems,” *Proc. IEEE Power Eng. Soc. Summer Meeting,* pp. 1645-1654, 2000.

[7] R. S. Al Abri, E. F. El-Saadany; Y. M. Atwa, “optimal placement and sizing method to improve the voltage stability margin in a distribution system using distributed generation,” *IEEE Trans. Power syst.,* vol. 28, 2013.

[8] P. Aristidou, G. Valverde, T. V. Cutsem, “Contribution of Distribution Network Control to Voltage Stability: A Case Study”, *IEEE Trans. Smart Grid,* 2017, vol. 8, no. 1, pp: 106 –116.

[9] R. A. Walling, R. Saint, R. C. Dugan, J. Burke, L. A. Kojovic, “Summary of Distributed Resources Impact on Power Delivery Systems”, *IEEE Trans. Power Del.,* vol. 23, no. 3, JULY 2008.

[10] D. Guiping, J. Xu, “A new index of voltage stability considering Distribution electricity network,” *IEEE Asia-Pac. Power Energy Eng. Conf.,* 2009.

[11] T. Van Custem, “voltage stability of electic powet systems,” *Springer Sci. Bus. Media,* vol. 441, 1998.

[12] K.Liu, W. Sheng, L. Hu, Y. Liu, X. Meng, D. Jia, “Simplified probabilistic voltage stability evaluation considering variable renewable distributed generation in distribution systems”, *IET Gener. Transm. Distrib.,* 2015, vol. 9, no. 12, pp. 1464–1473.

[13] X. Ran, S. Miao, “Probabilistic evaluation for static voltage stability for unbalanced three-phase distribution system”, *IET Gener. Transm. Distrib.,* 2015, vol. 9, no. 14, pp. 2050–2059.

[14] F. Namdari, L. Hatamvand, N. Shojaei, H. Beiranvand, “Simultaneous RPD and SVC Placement in Power Systems for Voltage Stability Improvement Using a Fuzzy Weighted Seeker Optimization Algorithm”, *J. Oper. Autom. Power Eng.,* vol. 2, no. 2, pp. 129-140, 2014.

[15] S. Derafshi Beigvand, H. Abdi, S. N. Singh, “Voltage stability analysis in radial smart distribution grids,” *IET Gener. Transm. Distrib.,* vol. 11 no. 15, pp. 3722-3730, 2017.

[16] M. Chakravorty, D. Das, “Voltage stability analysis of radial distribution networks,” *Elsevier Sci. Ltd., Electr. Power Energy Syst.,* 23 (2001) 129-135.

[17] T. Zabaiou, L. A. Dessaint, I. Kamwa, “preventive control approach for voltage stability improvement using voltage stability constrained optimal power flow based on static line voltage stability indices,” *IET Gener. Transm. Distrib..,* vol. 8, pp. 924-934, 2014.

[18] M. Banejad, M. Kazeminejad, “Load effects on voltage stability in Distribution electricity network with considering of distributed generation,” *IEEE conf. 58th Int. Sci. conf. power Electr. Eng.,* 2017.

[19] K. A. Birt, J. J. Graffy, A. H. El-Abiad, “Three phase load flow program,” *IEEE Trans. Power App. Syst.,* vol. 95, no. 1, 1976.

[20] X. P. Zhang, “Fast three phase load flow methods,” *IEEE Trans. Power syst.,* vol. 11, no. 3, 1996.

[21] D. Singh, R. K. Misra, De. Singh, “Effect of load models in distributed generation planning,” *IEEE Trans. Power syst.,* vol. 22, no. 4, 2007.

[22] T. Gozel, M.H. Hocaoglu, U. Eminoglu, A. Balikci, “optimal placement and sizing of distributed generation on radial feeder with different static load models,” *Int. Conf. Future Power Syst.,* 2005.

[23] J. Machowski, “Power System Dynamics Stability and Control,” *John Wiley and Sons, Ltd, Second Edition*, 2008.

[24] IEEE Task Force on Load Representation for Dynamic Performance, “Bibliography on load models for power flow and dynamic performance simulation,” *IEEE Trans. Power syst., vol*. 10, 1995.

[25] IEEE Standard for Distributed Resoursec “Interconnected with Electric Power Systems,” *IEEE p1547 std.* 2002.

[26] R. A. Walling, et. Al. “Summary of distributed resources impact on power delivery systems,” *IEEE Trans. Power Del.,* vol. 23, no. 3, 2008.

[27] M. Abdel-Akher, “Voltage stability analysis of unbalanced distribution systems using backward/forward sweep load-flow analysis method with secant predictor”, *IET Gener. Transm. Distrib*., 2013, vol. 7, no. 3, pp. 309-317.

[28] A. Soroudi M. Ehsan, “Imperialist competition algorithm for distributed generation connections”, *IET Gener. Transm. Distrib.,* 2012, Vol. 6, Iss. 1, pp. 21–29.

[29] Musirin, T. K. Abdul Rahman, “On-Line Voltage Stability Based Contingency Ranking Using Fast Voltage Stability Index (FVSI),” *IEEE/PES Transm. Distrib. Conf. Exhibition,* Yokohama, Japan, 6-10 Oct. 2002.

[30] M.M. Aman, G.B. Jasmon, H. Mokhlis, A.H.A. Bakar, “Optimal placement and sizing of a DG based on a new power stability index and line losses”, *Elsevier Sci.Ltd., Electr. Power Energy Syst.,* vol. 43 pp.1296-1304, 2012.

[31] IEEE PES Distribution Systems Analysis Subcommittee Radial Test Feeders. http://sites.ieee.org/pestestfeeders/re-sources/ .